Neurobiology of Disease 47 (2012) 38–48

Contents lists available at SciVerse ScienceDirect

Neurobiology of Disease

journal homepage: www.elsevier.com/locate/ynbdi

Striatal NMDA receptors gate cortico-pallidal synchronization in a rat model of Parkinson's disease

Camila L. Zold *, Mariela V. Escande, Pablo E. Pomata [1], Luis A. Riquelme, M. Gustavo Murer

Neural Circuit Physiology Lab, Systems Neuroscience Section, Department of Physiology and Biophysics, School of Medicine, University of Buenos Aires, 2155 Paraguay St., Buenos Aires C1121ABG, Argentina

ARTICLE INFO

Article history:
Received 31 October 2011
Revised 6 March 2012
Accepted 10 March 2012
Available online 18 March 2012

Keywords:
Striatum
NMDA receptor
Parkinson's disease
Globus pallidus
Neuronal synchronization
Neuronal phase locking

ABSTRACT

Anomalous patterns of synchronization between basal ganglia and cortex underlie the symptoms of Parkinson's disease. Computational modeling studies suggest that changes in cortical feedback loops involving trans-striatal and trans-subthalamic circuits bring up this anomalous synchronization. We asked whether striatal outflow synchronizes globus pallidus neurons with cortical activity in a rat model of Parkinson's disease. We found that striatal firing is highly increased in rats with chronic nigrostriatal lesion and that this hyperactivity can be reduced by locally infusing a competitive NMDA receptor antagonist. Moreover, NMDA receptor-dependent striatal output had frequency dependent effects on distinct pathological patterns of cortico-pallidal coupling. Blockade of striatal NMDA receptors almost completely abolished an anomalous ~1 Hz cortico-pallidal anti-phase synchronization induced by nigrostriatal degeneration. Moreover, under striatal NMDA receptor blockade, synchronization with 2.5–5 Hz cortical oscillations falls to negligible levels and oscillations at 10–20 Hz are markedly attenuated, whereas beta synchronization (with a peak at ~26 Hz) is marginally reduced. Thus, tonic activation of striatal NMDA receptors allows different forms of anomalous oscillations along the cortico-striato-pallidal axis. Moreover, the frequency dependent effects of NMDA receptors suggest that low and high frequency parkinsonian oscillations stem from partially different mechanisms. Finally, our results may help to reconcile views about the contributions of changes in firing rate and oscillatory synchronization to Parkinson's disease symptoms by showing that they are related to each other.

Introduction

Excessive synchronization between basal ganglia and cortex is a hallmark of Parkinson's disease (Hammond et al., 2007). This synchronization may take oscillatory forms and spans a broad range of frequencies. Although several studies explored its correlation with clinical signs and its dopamine dependence, the underlying mechanisms remain unclear (Gittis et al., 2011; McCarthy et al., 2011; Moran et al., 2011; Rosin et al., 2011).

A recent study provided causal evidence linking the activity of striatal medium spiny projection neurons (MSNs) and parkinsonian-like behaviors in mice (Kravitz et al., 2010). Although that study links parkinsonism to hyperactivity in MSNs of the indirect pathway and hypoactivity in the direct pathway (Albin et al., 1989), it has been claimed that the "rate model" cannot explain how oscillatory synchronization in the basal ganglia circuit arises.

Medium spiny neuron firing is only possible during "up states", a close-to-threshold depolarized state sustained by synaptic inputs from the cortex and thalamus. We have found that up states in dorsal striatum MSNs are synchronized to cortical ensembles (Kasanetz et al., 2002; Tseng et al., 2001), and that a subgroup of MSNs shows more depolarized up states and an increased firing probability in rats with nigrostriatal lesion (Tseng et al., 2001). We proposed that an increased excitability of MSNs allows an exaggerated transmission of resting cortical rhythms through the striatum in the parkinsonian condition, allowing an anomalous representation of these rhythms downstream in the basal ganglia circuit (Tseng et al., 2001). Subsequent work by Mallet et al. (2006) has shown that MSNs most probably projecting to the globus pallidus (GP) are hyperactive in rats with nigrostriatal lesion. However, because GP firing rate may be normal, increased or decreased in animal models of Parkinson's disease, and not consistently decreased as could be predicted following the GABAergic nature of MSNs, the functional significance of hyperactivity in "indirect pathway MSNs" has been questioned. Alternative models have put emphasis on interactions between the subthalamic

* Corresponding author at: Johns Hopkins University, Department of Neuroscience, Wood Basic Science Building, 725 N Wolfe St., Rm. 914, Baltimore, MD 21205, USA.
E-mail addresses: czold@jhmi.edu, neurofis@fmed.uba.ar (C.L. Zold), pomata@dna.uba.ar (P.E. Pomata).
[1] Present address: Laboratorio de Microdisección Láser, Instituto de Biología y Medicina Experimental, Vuelta de Obligado 2490, C1428ADN Buenos Aires, Argentina.
Available online on ScienceDirect (www.sciencedirect.com).

0969-9961/$ – see front matter © 2012 Elsevier Inc. All rights reserved.
doi:10.1016/j.nbd.2012.03.022

nucleus and GP and on changes in the gain of the cortico-subthalamic pathway, in driving abnormal oscillatory activity in the GP (Bevan et al., 2002; Leblois et al., 2006; Mallet et al., 2008).

Previously we have found that chronic nigrostriatal lesion inverts the phase relationship between slow oscillations in the frontal cortex and neuronal firing in the GP (Zold et al., 2007a; see also Magill et al., 2001; Walters et al., 2007). Normally, when cortical output increases pallidal activity also increases, but instead, in rats with a chronic nigrostriatal lesion, half of the pallidal neurons show the opposite. We have proposed that this owes to a switch from cortical excitatory (cortico-subthalamo-pallidal) to inhibitory (cortico-striato-pallidal) dominance over the GP (Zold et al., 2007a). Here we ask whether enhanced firing of MSNs during the up state promotes the anomalous synchronization between the cortex and GP in the parkinsonian condition.

Materials and methods

All experimental procedures were in accordance with institutional (CICUAL, RS2079/2007, University of Buenos Aires) and government regulations (SENASA, RS617/2002, Argentina). Male adult Sprague–Dawley rats were maintained on a 12 h light:12 h dark cycle (lights on at 7.00 a.m.) with free access to food and tap water. Rats weighting 190–220 g received an injection of 6-hydroxydopamine (6-OHDA) hydrobromide in the medial forebrain bundle, unilaterally, according to published protocols (Zold et al., 2007a). Control rats were injected with vehicle. All 6-OHDA-lesioned rats included in the present study exhibited a severe deficit in the use of the contralateral forelimb and an almost complete depletion of dopamine neurons in the substantia nigra (Zold et al., 2007b).

In vivo electrophysiology

In all experiments spiking activity in the striatum and/or GP was recorded simultaneously with the frontal cortex electrocorticogram (ECoG), 4–8 weeks post-lesion, following procedures described in Zold et al. (2007a, 2007b). Briefly, rats were anesthetized with urethane (1.2–1.5 g/kg, i.p.), treated with a local anesthetic in the scalp and pressure points (bupivacaine hydrochlorate solution, 5% w/v, 0.1–0.3 ml) and secured to a stereotaxic frame. Temperature was maintained between 36 and 37 °C with a servo-controlled heating pad. Additional urethane was administered as required to retain an abolished reflex response to a tail pinch (customarily 0.1 to 0.2 g/kg i.p. every 2 to 4 h). A concentric bipolar electrode (SNE-100, Better Hospital Equipment, Rockville Centre, NY, U.S.A.) positioned in the frontal cortex (3.2 mm anterior to bregma, 1.5 mm from midline and 2 mm from cortical surface; Paxinos and Watson, 1997) was used to obtain a differential frontal cortex local field potential recording (0.1–300 Hz bandwidth) (Zold et al., 2007a). In some experiments an additional SNE-100 electrode was positioned in the mesopontine tegmentum (1 mm anterior to lambda, 2.0 mm from midline, 7.5 mm below cortical surface) to allow performing bipolar electrical stimulation (200–800 μA, 300 μs square pulses in 50 Hz trains lasting 0.3–0.5 s) to induce episodes of cortical "activation" as described in Kasanetz et al. (2002). Extracellular recordings of striatum (1–1.5 mm anterior to bregma, 2.5–3 mm from midline, 5.5–6 mm below cortical surface) or striatum and GP (0.8–1.2 mm caudal to bregma, 5–5.5 mm from midline with a 20º angle in the coronal plane, 4–6 mm from brain surface) were taken with multi-channel silicon probes (32 channels, two-shanks 500 μm apart; NeuroNexus Technologies, Ann Arbor, MI, U.S.A.). In experiments studying the slow wave state we sampled 16 channels with 200 μm vertical site spacing and in experiments studying the cortical activated state we sampled 24 channels with 100 μm vertical site spacing. The signals (300–3000 Hz) were digitized at 25 kHz together with the cortical local field potential. Spike sorting was performed as described in Zold et al. (2007a, 2007b) by using *wave_clus* (Quiroga et al., 2004).

Pharmacology

To determine whether striatal NMDA receptors regulate striatal and pallidal firing, we infused in the striatum a competitive NMDA receptor antagonist through reverse microdialysis as described in previous studies (Pomata et al., 2008). A microdialysis probe (4 mm of exposed membrane; Bioanalytical Systems) was vertically inserted into the striatum (1.5 mm anterior to bregma, 2.5–3 mm from midline, 5.5–6 mm below cortical surface) and perfused at 2 μl/min with artificial cerebrospinal fluid (ACSF). A precision switch with zero dead space allowed perfusing the cannula with either ACSF or ACSF containing drug. The composition of ACSF was (in mM): 147 NaCl, 3 KCl, 0.8 MgCl, 1.2 $CaCl_2$, 2.0 NaH_2PO_4, and 2.0 Na_2HPO_4; osmolarity: 290–300 mOsm/L; pH 7.4 (Pomata et al., 2008). After recording baseline activity during ACSF infusion, we studied the effect of the competitive NMDAR antagonist D-(−)-2-amino-5-phosphonopentanoic acid (AP-5; Tocris, Minneapolis, MN, USA), 100 or 200 μM, on striatal and pallidal activity.

Data analysis

The prevalent global brain state under urethane is characterized by slow waves in the cortex and resembles closely slow wave sleep (Kasanetz et al., 2002; Mahon et al., 2006). Synchronization between spiking activity of pallidal neurons and slow waves in the ECoG was assessed by using spectral analysis followed by coherence and phase estimation, as in Zold et al. (2007a). A significant coherence (higher than $1-(0.05)^{1/L-1}$, where L = number of segments) at the dominant frequency of the cross-spectrum was taken as the primary criterion of oscillatory synchronization (Halliday et al., 1995). To determine the relationship between spike discharges and higher frequency components of the ECoG in the activated state, the ECoG was decomposed with a discrete wavelet transform (Meyer type) to obtain the following band-passed waveforms: 0.2–2.5 Hz, 2.5–5 Hz, 5–10 Hz, 10–20 Hz, 20–40 Hz, and 40–80 Hz. The frequency cuts were chosen based on the spectral composition of the ECoG in 6-OHDA rats (Suppl. Fig. 1). As a filter, wavelet decomposition compares well to other digital filtering algorithms (14–22 dB/octave attenuation depending on the band, e.g., 15.2 dB/octave at the 20 Hz cut and 21.3 dB/octave at the 40 Hz cut). A Hilbert transform was used to obtain the phase angle at every point of each waveform ("instantaneous phase") (see Galiñanes et al., 2009 and Zold et al., 2007b for further details). Next, the number of spikes occurring at different phase angles of each waveform was depicted in circular plots (bin size: 7.2°). Phase locking of spike discharges to a given frequency band was determined by assessing deviation from uniformity in these circular plots with the Rayleigh test. The strength of synchronization was further assessed by comparing the module of the resultant vectors summarizing these circular distributions (Fisher, 1993). In all phase and polar plots, 0° indicates the peak of the oscillation, and as a reference, the active part of the slow wave would peak at 0° in the current recordings as in our previous reports (Zold et al., 2007a, 2007b).

Post-mortem histology and immunohistochemistry

At the end of experiments, rats were given a high dose of urethane and transcardially perfused with saline containing heparin (500 UI/l) followed by 4% paraformaldehyde in phosphate-buffer (PB). Coronal sections (40 μm thick) were obtained throughout the substantia nigra, GP, anterior striatum and frontal pole in a microtome equipped with a freezing stage. Electrodes and microdialysis cannulae positions

were established in tissue sections stained with Safranine O (MP Biomedicals, Irvine, CA, U.S.A.). The position of the multichannel electrode was determined by visualization of a fluorescent dye left along the electrode track (DiI, Invitrogen). The extent of 6-OHDA-induced nigrostriatal damage was confirmed by immunohistochemical detection of tyrosine hydroxylase (TH) on sections from the anterior striatum and substantia nigra as described in Zold et al., 2007a, 2007b. All 6-OHDA-lesioned rats included in the present study exhibited a severe deficit in the use of the contralateral forelimb and a severe depletion of dopamine neurons in the substantia nigra.

Results

NMDA receptor-dependent striatal output in parkinsonian rats

Local administration of an NMDA receptor antagonist reduces up state amplitude by a few millivolts and decreases spontaneous firing in MSNs in normal rats (Pomata et al., 2008). To determine if striatal output is also modulated by NMDA receptors in parkinsonism, we studied the effect of local NMDA receptor blockade on striatal multiunit activity in 6-hydroxydopamine (6-OHDA) rats. The rat 6-OHDA lesion model reproduces the more marked denervation of the motor dorsolateral—compared to the ventromedial-striatum and some of the core behavioral deficits of Parkinson's disease (Cenci et al., 2002). Moreover, it has good predictive validity for the antiparkinsonian efficacy of drugs as well as for their potential to induce dyskinesia, a common complication of antiparkinsonian therapy (Cenci et al., 2002). Thus, despite its limited etiological validity, the rat 6-OHDA lesion model is well suited for studying the mechanisms underlying functional changes in the basal ganglia circuit in Parkinson's disease.

Seen through a multichannel electrode located at a pre-established stereotaxic position in the dorsal striatum (Fig. 1A), the total number of spikes per second produced by striatal neurons was several-fold higher in the parkinsonian striatum compared to sham controls, regardless of global brain state (Figs. 1B and C). In the slow wave state, multiunit spiking activity was five times higher in 6-OHDA rats (sham: 1.3 ± 0.2 vs 6-OHDA: 6.7 ± 0.5 spikes/s per channel, $p<0.00001$, t-test; 238 and 159 channels in 4 and 5 rats respectively). In three of the sham and three of the 6-OHDA rats in which multiunit activity could be evaluated during brain activation, the lesion induced a 3.5 fold increase in striatal activity (sham: 1.7 ± 0.4 vs 6-OHDA: 5.6 ± 1.3 spikes/s per channel, $p<0.01$, t-test; 70 and 56 recording channels, respectively). This is probably an underestimation of the real increase in striatopallidal outflow, because striatonigral neurons fire as much spikes as striatopallidal neurons in normal rats but are silent in the rat 6-OHDA lesion model (Ballion et al., 2009; Mallet et al., 2006).

The difference between control and 6-OHDA rats is also noticeable at the level of single units. In the slow wave state the average firing rate of striatal units was 0.71 ± 0.10 spikes/s in sham rats compared to 2.2 ± 0.24 spikes/s in 6-OHDA rats ($n=63$ and 82 respectively, $p=7.9E-08$, t-test; Suppl. Fig. 1). In the activated ECoG condition, single unit firing rates were 1.3 ± 0.49 ($n=26$) and 3.3 ± 0.75 ($n=22$) spikes/s in sham and 6-OHDA rats respectively ($p=0.038$). The less impressive effect of the lesion on single unit firing than multiunit activity reflects that spike sorting is biased against the selection of slowly firing units and that not all detected spikes can be attributed to a unit. Moreover, more units may be contributing to multiunit activity in 6-OHDA rats than controls. This is consistent with the higher percentage of silent striatal recording sites in sham than 6-OHDA rats (16% and 4% respectively, $p<0.0001$, Fisher exact test). Thus, multiunit activity

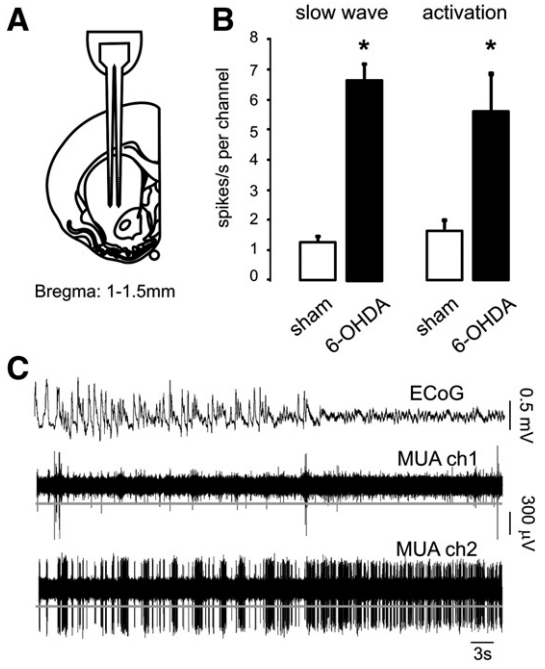

Fig. 1. Striatal hyperactivity in rat parkinsonism. A. Unbiased estimate of striatal hyperactivity obtained through a multichannel electrode located in a pre-established position in the striatum. The electrode was lowered into the striatum to record multiunit spiking activity during 10 min in four control and five 6-OHDA rats. Most of the recorded activity was with the rats in the slow wave state, but in three rats of each group multiunit activity could also be evaluated in the activated state condition. B. The number of spikes recorded per channel per second was significantly higher in 6-OHDA rats than controls both in the slow wave state ($p<0.00001$, t test) and the activated brain condition ($p<0.01$. t test). C. Representative traces showing the ECoG and two multiunit activity channels (MUA) in a transition to the activated state in a 6-OHDA rat. The gray lines are the thresholds used for spike detection.

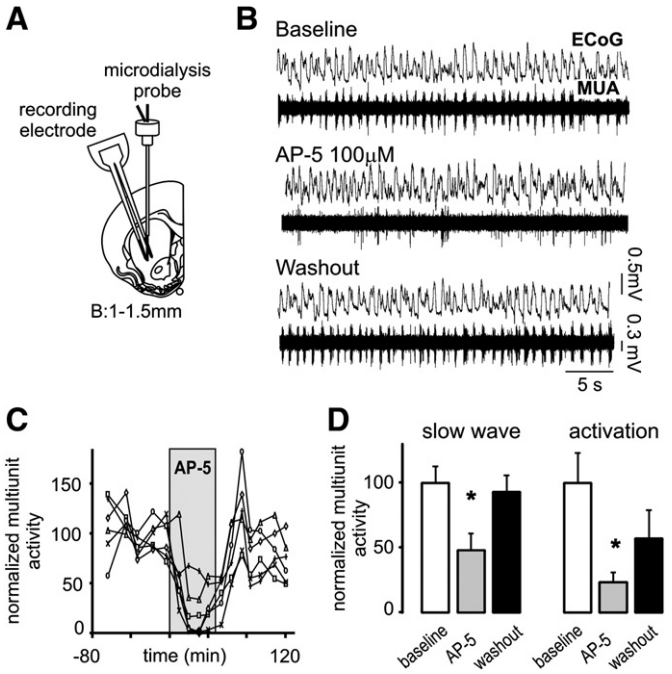

Fig. 2. NMDA receptor-dependent striatal outflow in 6-OHDA rats. A. Striatal activity was recorded through 16 channels of a multichannel electrode located 0.5–1 mm from a microdialysis probe in the striatum of six 6-OHDA rats. B. Representative traces showing multiunitary activity (MUA) in one channel before, during and after the infusion of AP-5 (100 µM) by reverse microdialysis, with the corresponding electrocorticographic (ECoG) traces (slow wave state). C. Time course of multiunit activity in several channels in a representative experiment. Each data point corresponds to 3 min of normalized multiunit activity. D. Intrastriatal AP-5 reduced in a reversible manner striatal output in 6-OHDA rats ($p<0.01$, repeated measures ANOVA). Data are mean ± SEM obtained from six rats in the slow wave state and three rats in the activated condition.

provides a more complete estimation of striatal output than the firing rate of single units.

To determine the contribution of NMDA receptors to striatal output, we recorded multiunit activity through 16 channels of an electrode located near a microdialysis probe in the striatum of a new group of six 6-OHDA rats (Fig. 2A). In the slow wave state (Fig. 2B), infusion of the competitive NMDA receptor antagonist AP-5 (100 μM) reduced striatal multiunit firing by 54% in 6-OHDA rats at sites located less than 1 mm from the microdialysis probe (Figs. 2C–D), without having any effect on striatal multiunit activity at 2 mm from the probe (baseline: 4.8 ± 0.6; AP-5: 4.2 ± 0.7 spikes/s per channel, N.S., repeated measures ANOVA), indicating a local effect of AP-5. Moreover, in three of the rats in which we could test the effect of AP-5 during brain activation, AP-5 reduced striatal multiunit firing by 77% (Fig. 2D). Thus, striatal outflow depends on local NMDA receptor stimulation both in normal rats (Pomata et al., 2008) and after chronic nigrostriatal lesion (Fig. 2).

Resting pallidal activity is independent of striatal output in normal conditions

In slices, GP neurons respond to inhibitory input with a brief pause and a reset of their intrinsic pacemaker rhythm (Chan et al., 2004; Stanford, 2003). Consistent with a pacemaker mechanism, GP neurons fire tonically and very regularly in vivo during the silent period of cortical slow waves (Zold et al., 2007a, 2007b), when cortical and

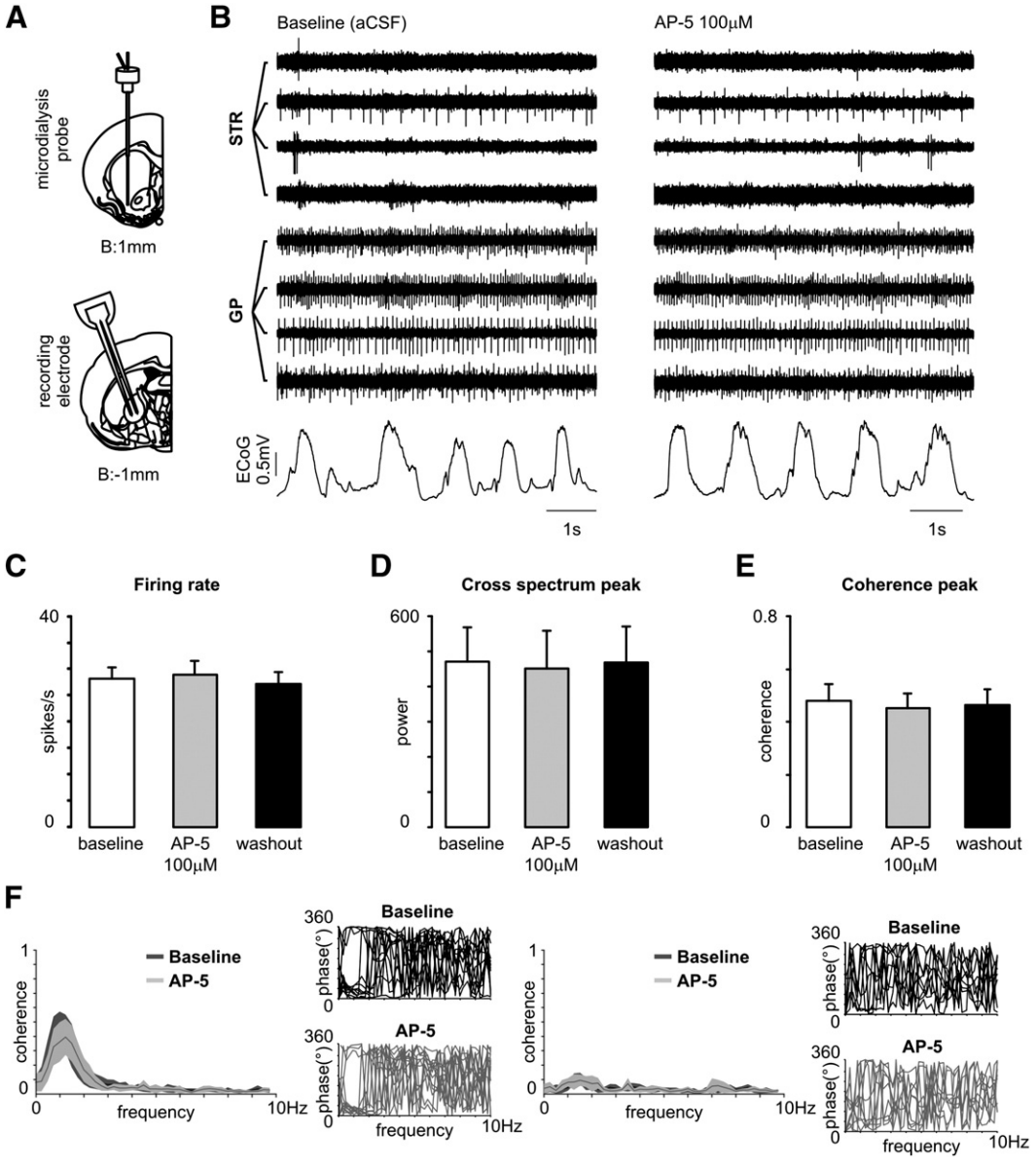

Fig. 3. Lack of striatal modulation of spontaneous pallidal activity in control rats. A. Drawings corresponding to coronal plates of the Paxinos and Watson atlas (1997) showing the location of a multichannel electrode in the GP and of a microdialysis probe in the striatum. Recordings were obtained from four control rats with the ECoG in the slow wave state. B. Representative traces showing pallidal (GP) and striatal (STR) activity before and during administration of AP-5 in the striatum, together with the ECoG, in a representative experiment. Note the in-phase modulation of some pallidal neurons (GP channels 2 and 3) by slow waves. Note also the lack of modulation by the slow waves of a tonically active striatal neuron, which are believed to be cholinergic interneurons (see Pomata et al., 2008). C. Firing rate of GP neurons before, during and after the administration of AP-5. Data are from 13 neurons identified by using a semiautomatic spike sorting algorithm. D and E. Cross-spectral power (D) and coherence (E) between GP firing and slow waves (0.8–1 Hz) showing no effect of AP-5 (NS, repeated measures). Data are mean ± SEM from at least 6 min of recording in each condition. F. Average coherence with 95% confidence interval and phase plots corresponding to pallidal single units showing in-phase (*left*, n = 13) or no modulation (*right*, n = 8) during slow waves. In the phase plots, each line corresponds to a single pallidal neuron and 0° at ~1 Hz indicates the peak of the slow wave (active part).

MSNs are in the down state and do not fire action potentials (Kasanetz et al., 2002). Cortical activity modulates GP neurons in control conditions, with pallidal neurons showing increased firing during the active part of the slow waves (Fig. 3; Zold et al., 2007a, 2007b). This is unlikely to be related to striatal input, which is inhibitory. To determine whether striatal output modulates the firing of GP neurons, we tested the effect of infusing AP-5 in the striatum on the activity of 21 pallidal single units individualized with a semiautomatic spike sorting algorithm in four rats. Thirteen of the neurons showed an in-phase modulation at the frequency of the slow waves (0.8–1 Hz) and eight neurons fired regularly without any significant modulation across the slow wave (Zold et al., 2007a, 2007b). Intrastriatal infusion of AP-5 (100 μM) had no effect on the activity of the thirteen pallidal in-phase neurons recorded in four normal rats (Fig. 3). Neither the firing rate nor the synchronization between the cortex and the GP was affected by NMDA receptor antagonist administration (firing rate: 28.2 ± 2.1 vs 28.9 ± 2.6 spikes/s; coherence: 0.5 ± 0.06 vs 0.48 ± 0.06 in baseline and AP-5 condition respectively, $p > 0.05$, repeated measures ANOVA). Moreover, the NMDA receptor antagonist did not modify the activity of the "non-modulated" pallidal neurons (coherence under ACSF: 0.12 ± 0.02, coherence under AP-5: 0.11 ± 0.02; firing rate under ACSF: 22.0 ± 1.9 spikes/s, firing rate under AP-5: 21.9 ± 2.1 spikes/s). Thus, in normal resting conditions, the striatum has little influence on spontaneous activity in the GP.

Anti-phase pallidal oscillations are driven by NMDA receptor-dependent striatal output

One of the most dramatic electrophysiological changes induced by chronic nigrostriatal damage in rats is an anti-phase synchronization between cortex and GP (Magill et al., 2001; Zold et al., 2007a). During slow waves, when the cortex and striatum show alternative periods of synchronized firing and silence, ~50% of the GP neurons reduce their firing when cortical activity increases in rats with nigrostriatal lesion (Zold et al., 2007a and Fig. 4A). Although this is consistent with our hypothesis that MSNs transmit an inhibitory cortical influence to the GP, alternative explanations are possible. For instance, the excitatory cortico-subthalamo-pallidal pathway could activate intrapallidal inhibition via local axon collaterals. However, intrastriatal infusion of AP-5 markedly attenuated or abolished anti-phase synchronization between cortex and GP without significantly changing the mean firing rate of the eighteen pallidal neurons tested (Fig. 4B; firing rate under ACSF: 34.2 ± 2.8; AP-5: 34.7 ± 2.7; washout: 32.6 ± 3.2 spikes/s; mean ± SEM, n = 18 neurons in 5 rats; $p > 0.05$, repeated measures ANOVA).

Synchronization was assessed with coherence, which is a normalized measure of linear correlation in the frequency domain which takes values between 0 and 1 (Halliday et al., 1995). Coherence attains its highest value when the phase shift and ratio between the powers of two waveforms remain constant. In the above eighteen

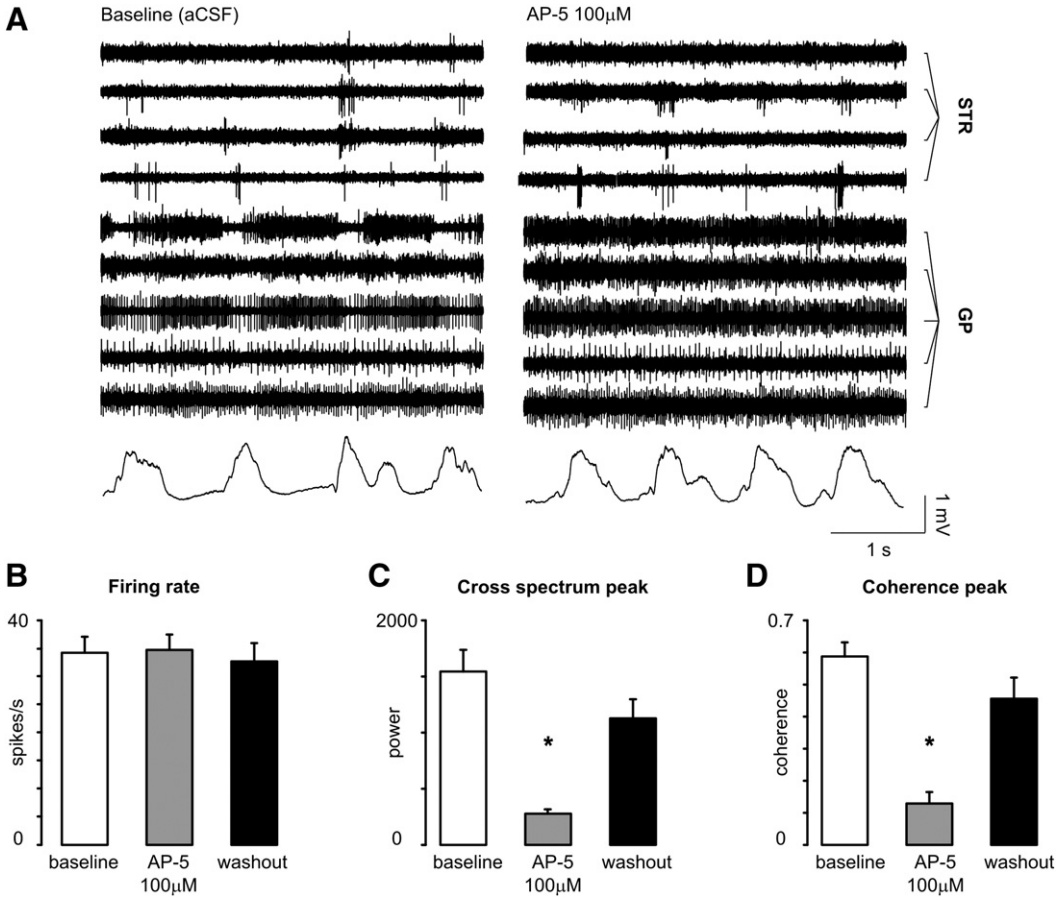

Fig. 4. Striatal dependence of anti-phase activity in the globus pallidus in parkinsonian rats. A. Representative traces showing pallidal and striatal activity before and during administration of AP-5 (100 μM) in the striatum of a 6-OHDA rat. Note the anti-phase modulation of some pallidal neurons by slow waves and the disappearance of anti-phase activity during administration of AP-5. B. Firing rate of anti-phase pallidal neurons before, during and after the administration of AP-5. Data are from 18 neurons identified by using a semi-automatic spike sorting algorithm. C and D. Cross-spectral power (C and coherence (D) at the peak frequency of slow waves (0.8–1 Hz) showing a reduction of anti-phase synchronization during administration of AP-5 ($p < 0.01$. repeated measures ANOVA). Data are mean ± SEM from at least 6 min of recording in each condition. Recordings were obtained from five 6-OHDA rats with the ECoG in the slow wave state.

pallidal neurons showing anti-phase coherence with cortical slow waves during continuous ACSF infusion, the administration of AP-5 (100 μM) turned coherence non-significant in 15 instances. On average, anti-phase coherence at slow wave frequency (0.8–1 Hz) was reduced by 78% during AP-5 infusion (Figs. 4C–D; coherence under ACSF: 0.59 ± 0.04; coherence under 100 μM AP-5: 0.13 ± 0.03, mean ± SEM, $p<0.001$ repeated measures ANOVA). In an independent group of three 6-OHDA rats in which another nine pallidal neurons showing anti-phase coherence with slow waves were studied, infusion of 200 μM AP-5 produced similar results (coherence at 0.8–1 Hz under ACSF: 0.55 ± 0.06, under 200 μM AP-5: 0.09 ± 0.04; washout: 0.4 ± 0.09; mean ± SEM, $p<0.01$, repeated measures ANOVA), and coherence was turned to non-significant values in all nine instances. Thus, in the parkinsonian condition, the striatum transmits a functionally effective cortical inhibitory influence to the GP, which can induce anomalous oscillatory activity without modifying the mean firing rate of pallidal neurons.

In addition to the above 27 anti-phase neurons, 18 pallidal neurons showing regular firing insensitive to slow waves ("non-modulated neurons") and 10 neurons showing in-phase increases in firing with slow waves could be studied in these experiments (data from experiments with 100 μM and 200 μM AP-5 were pooled for the analysis shown in Fig. 5). The activity of non-modulated neurons

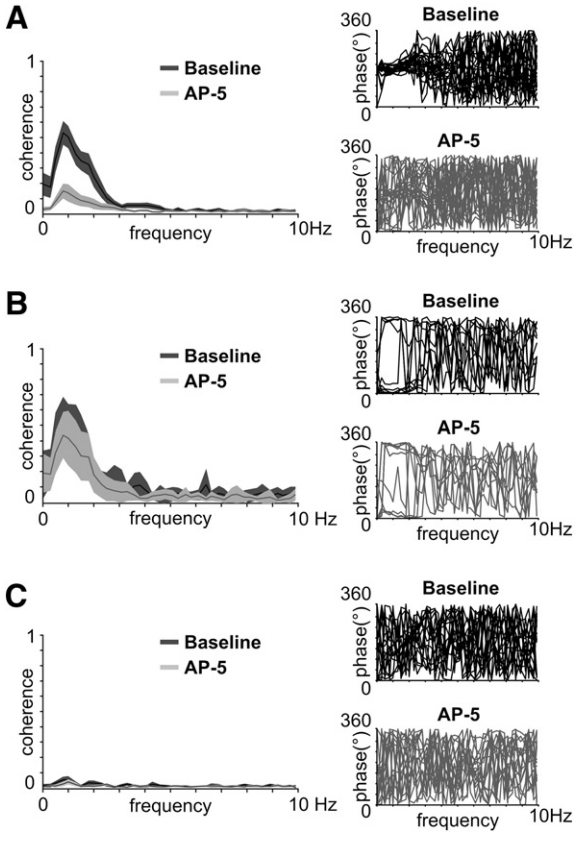

Fig. 5. Reduced pathological synchronization between cortex and globus pallidus during slow waves after intrastriatal administration of AP-5 to parkinsonian rats. Average coherence with 95% confidence interval (*left*) before and during AP-5 administration in pallidal single units showing different phase relationships with slow waves (*right*). Data from five rats treated with 100 μM AP-5 and three rats treated with 200 μM AP-5 have been pooled. In the phase plots, each line corresponds to a single pallidal neuron and 0° at ~1 Hz indicates the peak of the slow wave (active part). A. "Anti-phase neurons" showing a ~180° phase relationship with slow waves (minimum firing rate at the peak of the oscillation) show a marked reduction of coherence and loose the anti-phase relationship with the ECoG under AP-5 (n = 27 neurons). B. In-phase synchronization of pallidal neurons with slow waves (n = 10, ~0° phase angle at ~1 Hz under ACSF) is less sensitive to AP-5 administration. C. Non-modulated pallidal neurons (n = 18) show very low coherence with slow waves which is not modified by AP-5 infusion.

remained unchanged during intrastriatal AP-5 infusion (coherence under ACSF: 0.06 ± 0.01, coherence under AP-5: 0.05 ± 0.01; firing rate under ACSF: 22.9 ± 1.7 spikes/s, firing rate under AP-5: 22.2 ± 1.2 spikes/s), whereas that of in-phase neurons was marginally affected (coherence under ACSF: 0.58 ± 0.07, coherence under AP-5: 0.49 ± 0.08, $p = 0.02$, repeated measures ANOVA; firing rate under ACSF: 16.6 ± 2.9 spikes/s, firing rate under AP-5: 17.6 ± 3.2 spikes/s, NS). Overall, the data show a more marked striatal output dependency of anti-phase than in-phase slow wave modulation of pallidal firing.

Changes in pallidal activity during cortical activation also depend on striatal output

Slow waves are chains of up and down states with a frequency of ~1 Hz and are a hallmark of anesthesia and slow wave sleep (Steriade et al., 1993). During wakefulness up states are more persistent and irregular, but stem from the very same capacity of cortical networks of self-sustaining a depolarized state through a balance between excitation and inhibition (Destexhe et al., 2007). Up states dynamically similar to those observed in the awake state occur during anesthesia, both in the cortex and striatum (Mahon et al., 2006; Steriade et al., 2001). To determine whether striatal output drives oscillations in the parkinsonian GP during the condition known as "activated state", we induced this state under anesthesia by stimulating the mesopontine tegmentum (Kasanetz et al., 2002) while recording the ECoG and pallidal activity as described above. Synchronization was assessed by plotting the number of spike occurrences at every phase of different ECoG frequency components (Fig. 6A) and phase-locking was defined as deviation from uniformity in these circular distributions (Fig. 6B).

Synchronization of pallidal firing to the activated ECoG is increased in 6-OHDA rats across a wide range of frequencies (Table 1). The spike phase circular distributions were built from an average of 4594 ± 280 spikes per neuron (n = 59) and 4474 ± 312 spikes per neuron (n = 33; NS; mean ± SEM) in five control and five 6-OHDA rats respectively. Overall, 6-OHDA rats had significantly more pallidal neurons phase-locked to low frequency oscillations (2.5–5 Hz), 10–20 Hz oscillations and beta activity (with a peak at ~26 Hz) than control rats, regardless of how stringent the criterion to statistically assess circular non-uniformity was (Fig. 6C), whereas only a minority of pallidal neurons showed phase locking to 5–10 Hz and 40–80 Hz ECoG oscillations in both groups (Table 1). Additionally, the resultant vector length of spike phase circular distributions, across all data, was significantly different between 6-OHDA rats and controls at 2.5–5 Hz (control: $9.7\times10^{-3}\pm8\times10^{-4}$, 6-OHDA: $3.5\times10^{-2}\pm5\times10^{-3}$, $p=1.2\times10^{-9}$), 10–20 Hz (control: $1.01\times10^{-2}\pm1.1\times10^{-3}$, 6-OHDA: $1.55\times10^{-2}\pm2.5\times10^{-3}$, $p=0.02$) and 20–40 Hz (control: $1.5\times10^{-2}\pm1\times10^{-3}$, 6-OHDA: $3.1\times10^{-2}\pm4\times10^{-3}$, $p=0.00001$, t test). Thus, synchronization between pallidal firing and cortical rhythms in 6-OHDA rats is prominent at low and beta range frequencies. Importantly, pallidal coupling with these cortical rhythms in control rats was negligible, indicating a truly anomalous nature of cortico-pallidal synchronization in the parkinsonian condition.

Anomalous cortico-pallidal synchronization in the activated state was limited to pallidal neurons showing significant in-phase or anti-phase coherence with slow waves as reported by Mallet et al. (2008) (Fig. 7). Among eight neurons showing in-phase ~1 Hz modulations in the slow wave state that could be studied in the activated state, five showed significant phase-locking to beta and/or 2.5–5 Hz cortical oscillations. Moreover, fourteen of the seventeen neurons showing anti-phase synchronization with slow waves were phase-locked to beta and/or 2.5–5 Hz oscillations in the activated state condition. In all but three of the slow wave modulated neurons, beta synchronization occurred together with significant phase-locking to

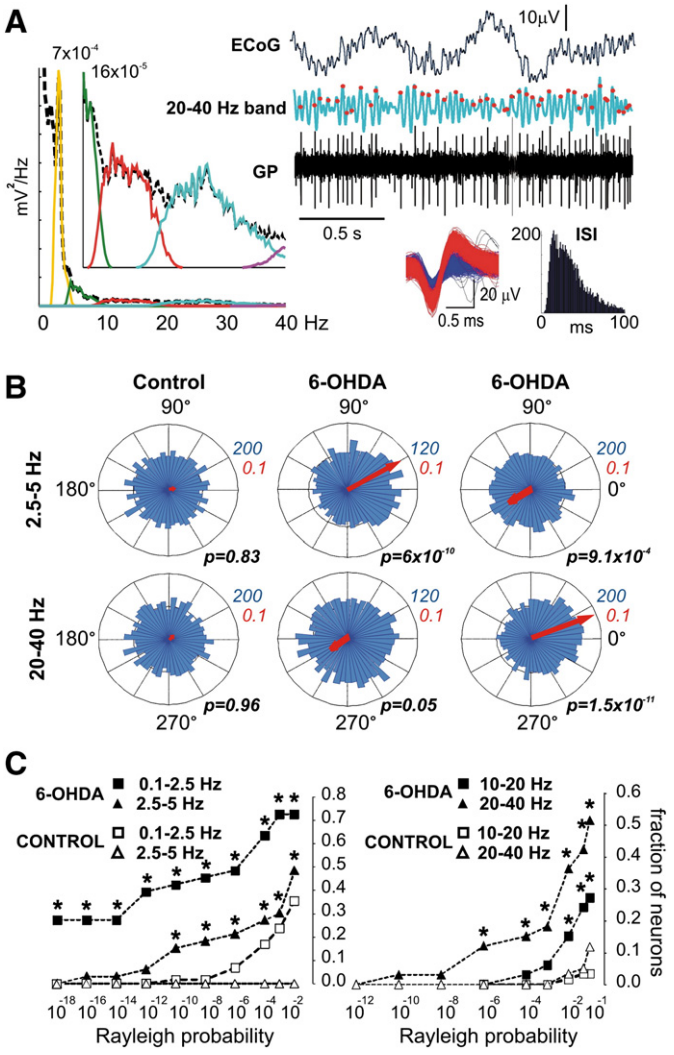

Fig. 6. Abnormal synchronization of pallidal firing with diverse cortical rhythms in parkinsonian rats. A. *Left:* Power spectrum of the activated ECoG (black dashed line) in a representative 6-OHDA rat and of the waveforms obtained through wavelet decomposition (yellow: 2.5–5 Hz, green: 5–10 Hz; red: 10–20 Hz; light blue: 20–40 Hz; purple: 40–80 Hz). Note the higher relative power of the low frequencies. The inset shows the high frequencies with an expanded scale. *Right:* Representative traces showing the activated ECoG, a waveform obtained by wavelet decomposition which retains the 20–40 Hz frequency components of the ECoG (light blue) and spike firing in a pallidal recording site. The red dots mark the occurrence of spikes in a pallidal neuron sorted from the signal shown above. Note the preferential occurrence of spikes at a distinct phase range of the beta oscillation. *Below:* Spike waveform (red) and interspike interval distribution of the pallidal neuron after sorting with *wave_clus*. B. Circular plots showing the number of spike occurrences (radial axis) as function of phase (circular axis) for low (2.5–5 Hz) and high (20–40 Hz) frequency components of the activated ECoG in a control pallidal neuron (left) and two different pallidal neurons recorded from 6-OHDA rats (which were "anti-phase" neurons according to their phase relationship with slow waves). 0° indicates the peak of the oscillation, and as a reference, the active part of the slow wave would peak at 0° in our recordings. The red arrows are the resultant vectors of each circular distribution. The red and blue numbers at the side of the polar plots are reference values of the radial axis for vector length (red) and spike occurrences per bin (blue). The control neuron does not show phase locking to either frequency (5400 spikes, 92 s of signal). The neuron in the middle shows a marked synchronization to the low frequency band (3913 spikes, 230 s) whereas that in the right (which is the same shown in A) shows high synchronization with the 20–40 Hz band and weak synchronization with the 2.5–5 Hz band (5477 spikes, 222 s). The *p* values were calculated with the Rayleigh test, which assesses deviation from uniformity in circular distributions. C. Proportion of neurons phase-locked to low (left) and high (right) frequencies of the activated ECoG, at increasing levels of deviation from circular uniformity as indicated by a lower *p* value in the Rayleigh test. At each significance level, the number of locked and non-locked neurons in control and 6-OHDA rats has been compared with the Fisher Exact Probability test (* $p<0.05$). Note that between-group differences are retained at more stringent significance levels in the low frequency range (Rayleigh *p* values of 10^{-8} and lower) than in the high frequency range (Rayleigh *p* values of up to 10^{-6}). Data are from 59 neurons recorded in five control rats and 33 neurons recorded in five 6-OHDA rats.

Table 1
Synchronization of pallidal spikes to the cortical local field potential in control and 6-OHDA rats.

	% neurons phase locked to each frequency band			Mean vector length, all neurons		
	Control	6-OHDA	*p*	Control	6-OHDA	*p*
0.1–2.5 Hz	55.9	78.8	0.04	0.029 ± 0.002	0.075 ± 0.009	<0.0001
2.5–5 Hz	0	57.6	<0.0001	0.010 ± 0.008	0.035 ± 0.005	<0.0001
5–10 Hz	0	0	N.S.	0.007 ± 0.001	0.010 ± 0.001	N.S.
10–20 Hz	3.4	24.2	0.004	0.010 ± 0.001	0.016 ± 0.003	N.S.
20–40 Hz	5.1	42.4	<0.0001	0.015 ± 0.001	0.031 ± 0.005	<0.0001
40–80 Hz	8.5	15.2	N.S.	0.014 ± 0.001	0.019 ± 0.002	N.S.

Data are from 59 control and 33 6-OHDA pallidal neurons recorded in the activated state condition of the ECoG. A neuron was considered phase locked if its spike phase circular distribution was non-uniform ($p<0.05$ in the Rayleigh test). Statistical comparisons have been done with the Fisher Exact Probability Test (contingency tables) or the t test (vector lengths).

2.5–5 Hz cortical oscillations. This supports previous findings showing alterations of cortical influence on a subset of GP neurons across different global brain states (Magill et al., 2001; Mallet et al., 2008; Zold et al., 2007b).

To determine if striatal NMDA receptors allow the influence of the activated ECoG on GP firing in 6-OHDA rats we assessed phase locking to different rhythms in 25 pallidal neurons before and during intrastriatal administration of 100 μM AP-5 (Fig. 8). We computed spike phase circular distributions (Fig. 8A) from an average of 11,839 ± 953 spikes per neuron under continuous ACSF and 10,820 ± 962 spikes per neuron during AP-5 infusion (mean ± SEM, $p=0.19$, paired t test). Modulation of pallidal firing by the low frequency components of the activated ECoG (2.5–5 Hz) was markedly reduced during AP-5 infusion. This was readily apparent as a significantly lower number of neurons showing non-uniform circular distributions (Fig. 8B) and a marked reduction of the resultant vector length of these distributions (62% length reduction; $p=0.0002$; Fig. 7C). Striatal NMDA receptor blockade had less marked effects on synchronization at higher frequencies. It reduced the number of neurons modulated by 10–20 Hz oscillations but not by a cortical beta rhythm with a peak at ~26 Hz (Fig. 8B). Moreover, resultant vector length was significantly reduced under AP-5 (Figs. 8C, 9), more markedly at 10–20 Hz (59%; $p=0.01$) than at 20–40 Hz (22%; $p=0.02$). Importantly, the effect of AP-5 on oscillations in the beta frequency range was independent of the cuts used to collect beta activity from the ECoG (Fig. 9 and Suppl. Fig. 2). Finally, in the activated state, intrastriatal AP-5 seemed to affect in an even manner neurons having in-phase and anti-phase synchronization with slow waves (Fig. 8C). Thus, intrastriatal AP-5 infusion reduced cortico-pallidal synchronization in 6-OHDA rats in a frequency dependent manner.

Discussion

Tonic stimulation of striatal NMDA receptors contributes to sustain a high striatal output in rats with chronic nigrostriatal lesion. In turn, striatal output induces an anomalous over-representation of resting cortical rhythms in the GP in parkinsonism. Consistent with the slow kinetics of NMDA receptor currents, striatal NMDA receptor stimulation contributes more to low frequency synchronization than to beta oscillations. Nevertheless, they have a significant influence on beta synchronization too.

Anomalous synchronization between the cortex and GP in the 6-OHDA rat spans a broad range of frequencies across different global brain states. We have previously described an anti-phase coupling of pallidal firing with frontal cortex slow waves in the 6-OHDA rats, and a more irregular firing pattern ("pausing") in the same neurons during ECoG activation, which are rarely seen under anesthesia in normal conditions (Zold et al., 2007a, 2007b). Here, by breaking down frontal cortex activity in complementary waveforms encompassing the whole frequency range of the resting ECoG, we demonstrate anomalous

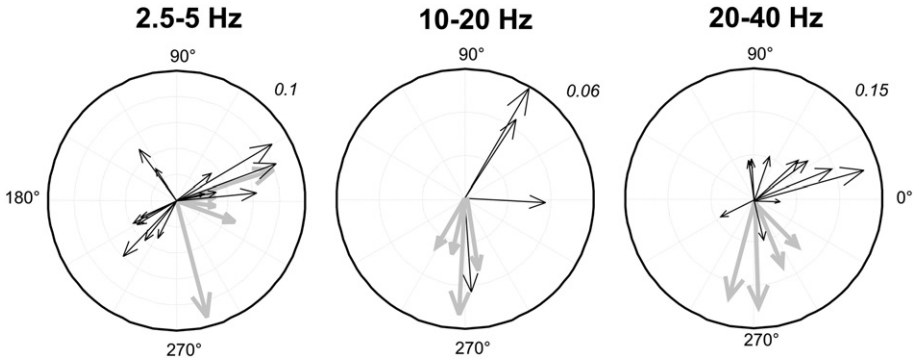

Fig. 7. Phase relationship of pallidal neurons with different rhythms of the activated ECoG in 6-OHDA rats. Each plot contains all neurons showing non-uniform spike phase circular distributions at $p<0.05$ significance in the Rayleigh test at the indicated frequency. The neurons were further divided in two groups based on their phase relationship with the ECoG in the slow wave state: black vectors correspond to anti-phase neurons, gray vectors to in-phase neurons. Among 33 neurons studied in the activated condition in 6-OHDA rats, 8 showed in-phase and 17 anti-phase locking to slow waves. The remaining 8 neurons that showed no slow wave modulation of firing, showed no significant phase-locking to any rhythm in the activated state. In the three polar plots, 0° indicates the peak of the oscillation, and as a reference, the active part of the slow wave peaks at 0° in the current recordings as in our previous reports (Zold et al., 2007a, 2007b). The radial axis (italics) indicates vector length. A test for equality of circular distributions (Kuiper two-sample test) shows that the in-phase (gray) and anti-phase (black) neurons do not separate out in two distributions at 2.5–5 Hz but they differ significantly at 20–40 Hz ($p=0.02$). The number of observations was too small to perform the test at 10–20 Hz.

cortico-pallidal synchronization at low (2.5–5 Hz), intermediate (10–20 Hz) and high frequencies (20–40 Hz), including beta oscillations peaking at ~26 Hz (see also Mallet et al., 2008; Zold et al., 2007b). This is in high contrast to control rats, which do not show any significant cortico-pallidal synchronization except for an in-phase modulation during slow waves (Zold et al., 2007a, 2007b). Excessive oscillatory activity at all these frequencies has been observed in neurons of the subthalamic nucleus and both pallidal segments in Parkinson's disease patients undergoing functional neurosurgery (Hutchison et al., 1997, 1998; Kühn et al., 2005; Levy et al., 2000, 2002; Moran et al., 2008; Rodriguez-Oroz et al., 2001) and in MPTP-lesioned monkeys (Bergman et al., 1994; Goldberg et al., 2004; Raz et al., 2000). Overall, these findings strengthen the validity of the rat 6-OHDA model for studying the pathophysiology of Parkinson's disease.

Previously, by combining reverse microdialysis to deliver NMDA receptor antagonists in the striatum with intracellular in vivo recordings, we have found that local NMDA receptor stimulation regulates firing probability in MSNs (Pomata et al., 2008). NMDA receptor blockade has frequency-dependent effects on the membrane potential of MSNs, inducing a reduction of low frequency modulations while sparing high frequencies, which may depend on fast glutamate- and GABA-mediated transmission. Although NMDA receptor blockade reduces striatal output in normal rats (Pomata et al., 2008), here we found that it does not modulate spontaneous activity in the GP. This is consistent with the small influence of resting cortical rhythms on GP firing in normal rats (see above). Overall, the data are consistent with the view that resting GP activity depends primarily on intrinsic pacemaker mechanisms and on the excitatory influence of the subthalamic nucleus in the dopamine intact brain (Chan et al., 2011; Magill et al., 2000).

In contrast, striatal NMDA receptor blockade reduced striatal hyperactivity and almost completely reversed low frequency cortico-pallidal synchronization in the parkinsonian condition. This was seen as an almost complete loss of anti-phase modulations during slow waves and a complete attenuation of low frequency (2.5–5 Hz) oscillatory synchronization in the activated ECoG condition. The effect of striatal output on low frequency synchronization is not limited to anti-phase synchronization, but extends to in-phase slow wave synchronization and to higher frequency oscillations taking place in in-phase neurons during the activated state. While the reduction of anti-phase synchronization between cortex and GP could be readily predicted following the inhibitory action of striato-pallidal synapses and previous work showing anti-phase synchronization between striatal and pallidal ensembles at low frequencies (Zold et al., 2007a), some of the observed effects could be secondary to changes in local interactions within the GP or in pallido-subthalamic communication. Importantly, the effect of striatal output on anomalous low frequency synchronization extends beyond the slow wave state. This is important given that resting low frequency oscillations in the EEG and corticostriatal BOLD signal are increased in patients with Parkinson's disease (Kwak et al., 2010; Stoffers et al., 2007).

Previous studies have shown that, in Parkinson's disease models, anomalous low frequency oscillations are coordinated along striatal, pallidal, subthalamic and basal ganglia output neurons (Dejean et al., 2008; Mallet et al., 2008; Walters et al., 2007; Zold et al., 2007a), and between neurons in all these structures and the cortex (Belluscio et al., 2003; Costa et al., 2006; Dejean et al., 2008; Gatev and Wichmann, 2009; Goldberg et al., 2004; Magill et al., 2001; Mallet et al., 2008; Tseng et al., 2001; Zold et al., 2007a, 2007b). Moreover, low frequency oscillatory firing associated with tremor has been observed in the thalamus in animal models and patients with Parkinson's disease (Guehl et al., 2003; Lenz et al., 1988) (note however that 6-OHDA rats do not show tremor). Our present results support the hypothesis that resting cortical rhythms spread abnormally through the striatum after nigrostriatal lesion, contributing to the over-representation of low frequency oscillations downstream of the striatum (Tseng et al., 2001). Recent modeling studies supported that an imbalance between feedback loops involving trans-basal ganglia pathways may bring on anomalous oscillatory synchronization along the whole basal ganglia circuit (Leblois et al., 2006). However, this study was focused on a fast trans-subthalamic loop rather than on the indirect pathway. Although the role of re-entrant mechanisms and interactions with other trans-basal ganglia pathways remains to be elucidated, our data show that low frequency cortico-pallidal synchronization depends on striatal output in the parkinsonian condition.

The contribution of the striatum to pathological beta oscillations is less clear. Previous studies suggesting that striatal hyperactivity is limited to the slow wave state (Mallet et al., 2006), supported the proposal that pallido-subthalamic beta oscillations stem from local network interactions (Bevan et al., 2002) and circuit loops faster than the indirect pathway (Bevan et al., 2002; Leblois et al., 2006). At difference with Mallet et al. (2006), but in line with our previous observations in a small sample of intracelullarly recorded MSNs (Kasanetz et al., 2002), we found that striatal hyperactivity extends to the activated state condition. Moreover, recent computational modeling studies propose that striatal input modulates pallido-subthalamic beta (Moran et al., 2011) or even that beta can be originated within the striatum (Gittis et al., 2011; McCarthy et al., 2011).

Although our data show that striatal NMDA receptor blockade reduces cortico-pallidal beta coupling, synchronization in the beta

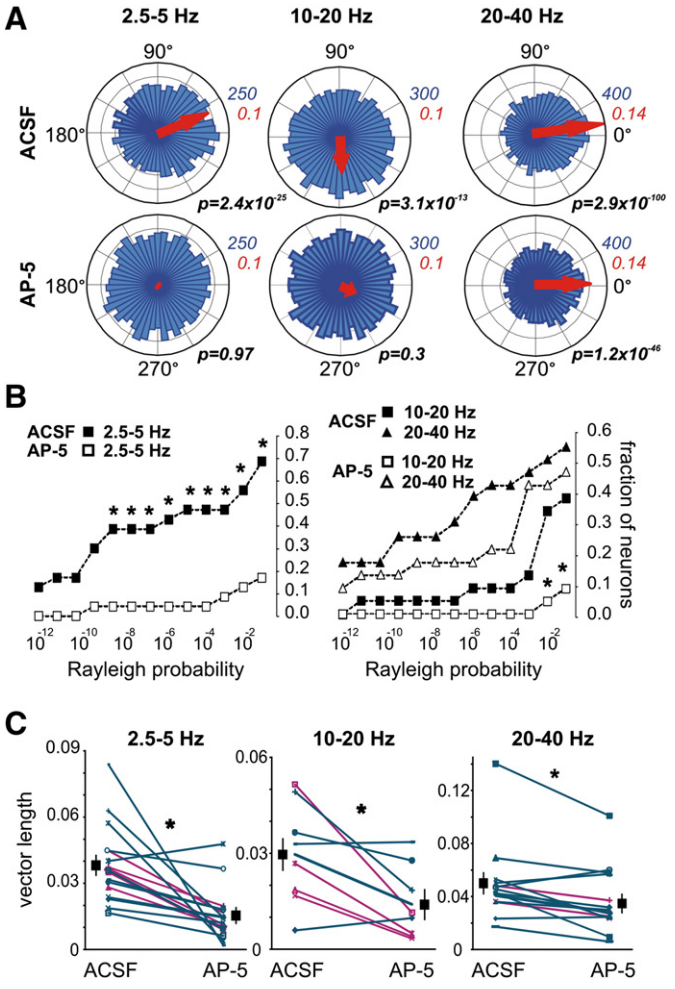

Fig. 8. Decoupling of pallidal firing from cortical rhythms in the activated state during striatal NMDA receptor blockade in parkinsonian rats. A. Circular plots showing the number of spike occurrences (radial axis) as function of phase (circular axis) corresponding to three pallidal neurons showing synchronization with 2.5–5 Hz (left), 10–20 Hz (middle) and 20–40 Hz (right) cortical rhythms in the activated state during baseline (ACSF), which was reduced under AP-5 infusion (100 μM). 0° indicates the peak of the oscillation, and as a reference, the active part of the slow wave would peak at 0° in our recordings. The red arrows are the resultant vectors of each circular distribution. The red and blue numbers at the side of the polar plots are reference values of the radial axis for vector length (red) and spike occurrences per bin (blue). The neuron in the middle showed in-phase synchronization with slow waves, the other two neurons were in anti-phase to the slow wave state. B. Proportion of neurons phase-locked to low (left) and beta (right) frequencies of the activated ECoG, at increasing levels of deviation from circular uniformity, under ACSF and during intrastriatal infusion of 100 μM AP-5. At each Rayleigh test significance level (x axis), the number of locked and non-locked neurons has been compared with the Fisher Exact Probability test (*$p<0.05$). Data are from 25 neurons recorded in five 6-OHDA rats. C. Effect of intrastriatal AP-5 (100 μM) on resultant vector length at each frequency band of the activated ECoG. For each band, all neurons showing circular distributions with significant deviation from uniformity at the $p<0.05$ significance level (Rayleigh test) are shown during baseline (ACSF) and under AP-5. Black squares are mean resultant vector lengths, and error bars, SEM. *$p<0.05$, paired t test. Neurons that showed in-phase synchronization with slow waves are marked with red lines, neurons in anti-phase with slow waves, with blue lines.

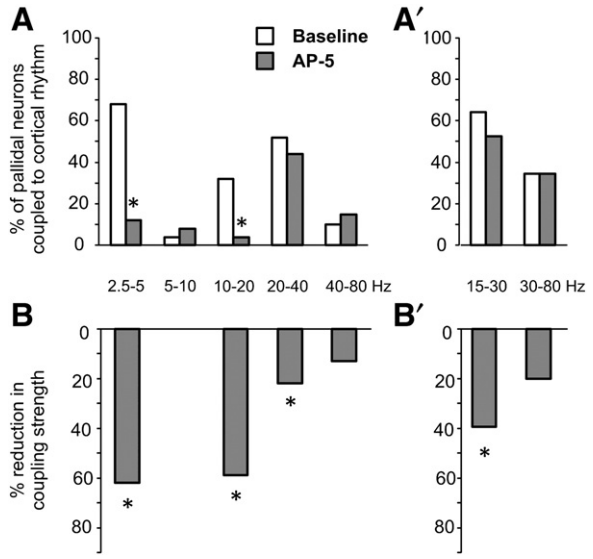

Fig. 9. Summary of the effects of striatal NMDA receptor blockade on anomalous cortico-pallidal synchronization in the activated cortical state condition. A. Proportion of coupled neurons before (ACSF) and during intrastriatal infusion of the NMDA receptor antagonist AP-5 in 6-OHDA rats with the ECoG in the activated state. B. Percent decrease in vector length at different frequencies after AP-5 intrastriatal administration in the same 6-OHDA rats. A' and B' show the same data analyzed with different frequency cuts to show that the effect of AP-5 in the beta range is independent of the frequency range selected for analysis. Data are the same used in Fig. 7. Phase locked neuron percentages were derived with $p<0.05$ in the Rayleigh test and coupling strength from changes in vector length (n = 25 neurons recorded in five 6-OHDA rats, *$p<0.05$).

range remains substantially elevated under AP-5. Because intrastriatal infusion of AP-5 did not abolish but only reduced MSN firing, and part of the striatum escaped from AP-5 effect, striatal influence on beta coupling could be more important than suggested by our findings. Moreover, the preferential effect of the NMDA receptor antagonist on the low frequency membrane potential oscillations of MSNs (Pomata et al., 2008) could have spared striatal influence on beta activity. Computational modeling studies suggested that changes in fast inhibitory local networks (Gittis et al., 2011) and an increased cholinergic activity (McCarthy et al., 2011) may enhance striatal beta synchronization in chronic dopamine depletion. In line with this view, LFP beta oscillations are increased in the striatum of rodents with severe striatal dopamine depletion (Costa et al., 2006; Moran et al., 2011). However, whether beta activity is encoded or not in striatal output in parkinsonism remains to be determined. Alternatively, an increased tonic striatal output may enhance or allow beta synchronization within the pallido-subthalamic network, as suggested by other computational modeling studies (Kumar et al., 2011; Terman et al., 2002). Although the ultimate mechanism through which striatal activity contributes to beta oscillations remains to be determined, our data show that striatal hyperactivity strengthens cortico-pallidal beta synchronization in chronic parkinsonism.

An important finding of the present study is the tonic contribution of NMDA receptor stimulation to striatal firing in the chronic parkinsonian condition. Previously we found that spontaneously active MSNs show more depolarized up states in rats with chronic nigrostriatal lesion (Tseng et al., 2001). Depolarization and tonic NMDA receptor stimulation may interact positively to enhance striatal output and corticostriatal synapse strength in indirect pathway MSNs. In normal conditions D2 receptor stimulation may counterbalance this positive feedback loop by inhibiting NMDA receptor currents and promoting endocannabinoid release and LTD (Higley and Sabatini, 2010; Kreitzer and Malenka, 2007; Liu et al., 2006; Shen et al., 2008), but chronic dopamine depletion may break down this balance resulting in an enhanced cortico-striato-pallidal axis. In turn, hyperactivity in indirect pathway MSNs may trigger compensatory mechanisms, like the pruning of dendritic spines and sprouting of inhibitory synapses (Day et al., 2006; Gittis et al., 2011), which may attenuate to some extent striatal hyperactivity. However, these homeostatic mechanisms may also have deleterious effects, by reducing integration of excitatory inputs and promoting fast oscillations in MSNs (Day et al., 2006; Gittis et al., 2011).

One influential theory about striatal function proposes that MSNs implement a gating mechanism that allows specific information flow through the striatum. According to the theory, a set of excitatory inputs

drives MSNs into a depolarized "up state" that allows them to fire in response to more specific, salient inputs. Although in the original statement and subsequent updates the theory refers to the nucleus accumbens (Gruber et al., 2009; O'Donnell and Grace, 1995), MSNs in the dorsal striatum may behave very similarly (Stern et al., 1998), even though other inputs may be more relevant to their function. We have proposed that up states in the dorsal striatum constitute a subthreshold representation of resting cortical firing patterns across different global brain states (Kasanetz et al., 2002). In this context, gating in the dorsal striatum may be understood as the ability of MSNs to sort out salient cortical inputs from the more global cortical firing pattern they are embedded in. This ability may be lost in the indirect pathway in Parkinson's disease, allowing the spreading of resting cortical rhythms along the cortico-striato-pallidal axis.

Acknowledgments

We thank Mariano Belluscio for helping with the 6-OHDA lesions and Dr. Juan Belforte (Universidad de Buenos Aires) for his comments on an early version of the manuscript. This study was supported by Secretaría de Ciencia, Tecnología e Innovación Productiva, Fondo para la Investigación Científica y Tecnológica, Argentina (PICT2007-05-01000, PICT2008-05-2205, PME2003-29), Universidad de Buenos Aires, Argentina (UBACYT 2011–2014 562), and Consejo Nacional de Investigaciones Científicas y Técnicas, Argentina (PIP0077).

Appendix A. Supplementary data

Supplementary data to this article can be found online at doi:10.1016/j.nbd.2012.03.022.

References

Albin, R.L., Young, A.B., Penney, J.B., 1989. The functional anatomy of basal ganglia disorders. Trends Neurosci. 12, 366–375.
Ballion, B., Frenois, F., Zold, C.L., Chetrit, J., Murer, M.G., Gonon, F., 2009. D2 receptor stimulation, but not D1, restores striatal equilibrium in a rat model of Parkinsonism. Neurobiol. Dis. 35, 376–384.
Belluscio, M.A., Kasanetz, F., Riquelme, L.A., Murer, M.G., 2003. Spreading of slow cortical rhythms to the basal ganglia output nuclei in rats with nigrostriatal lesions. Eur. J. Neurosci. 17, 1046–1052.
Bergman, H., Wichmann, T., Karmon, B., DeLong, M.R., 1994. The primate subthalamic nucleus. II. Neuronal activity in the MPTP model of parkinsonism. J. Neurophysiol. 72, 507–520.
Bevan, M.D., Magill, P.J., Terman, D., Bolam, J.P., Wilson, C.J., 2002. Move to the rhythm: oscillations in the subthalamic nucleus-external globus pallidus network. Trends Neurosci. 25, 525–531.
Cenci, M.A., Whishaw, I.Q., Schallert, T., 2002. Animal models of neurological deficits: how relevant is the rat? Nat. Rev. Neurosci. 3, 574–579.
Chan, C.S., Shigemoto, R., Mercer, J.N., Surmeier, D.J., 2004. HCN2 and HCN1 channels govern the regularity of autonomous pacemaking and synaptic resetting in globus pallidus neurons. J. Neurosci. 24, 9921–9932.
Chan, C.S., Glajch, K.E., Gertler, T.S., Guzman, J.N., Mercer, J.N., Lewis, A.S., Goldberg, A.B., Tkatch, T., Shigemoto, R., Fleming, S.M., Chetkovich, D.M., Osten, P., Kita, H., Surmeier, D.J., 2011. HCN channelopathy in external globus pallidus neurons in models of Parkinson's disease. Nat. Neurosci. 14, 85–92.
Costa, R.M., Lin, S.C., Sotnikova, T.D., Cyr, M., Gainetdinov, R.R., Caron, M.G., Nicolelis, M.A., 2006. Rapid alterations in corticostriatal ensemble coordination during acute dopamine-dependent motor dysfunction. Neuron 52, 359–369.
Day, M., Wang, Z., Ding, J., An, X., Ingham, C.A., Shering, A.F., Wokosin, D., Ilijic, E., Sun, Z., Sampson, A.R., Mugnaini, E., Deutch, A.Y., Sesack, S.R., Arbuthnott, G.W., Surmeier, D.J., 2006. Selective elimination of glutamatergic synapses on striatopallidal neurons in Parkinson disease models. Nat. Neurosci. 9, 251–259.
Dejean, C., Gross, C.E., Bioulac, B., Boraud, T., 2008. Dynamic changes in the cortex-basal ganglia network after dopamine depletion in the rat. J. Neurophysiol. 100, 385–396.
Destexhe, A., Hughes, S.W., Rudolph, M., Crunelli, V., 2007. Are corticothalamic 'up' states fragments of wakefulness? Trends Neurosci. 30, 334–342.
Fisher, N.I., 1993. Statistical Analysis of Circular Data/N.I. Fisher. Cambridge University Press, New York.
Galiñanes, G.L., Taravini, I.R., Murer, M.G., 2009. Dopamine-dependent periadolescent maturation of corticostriatal functional connectivity in mouse. J. Neurosci. 29, 2496–2509.
Gatev, P., Wichmann, T., 2009. Interactions between cortical rhythms and spiking activity of single basal ganglia neurons in the normal and parkinsonian state. Cereb. Cortex 19, 1330–1344.
Gittis, A.H., Hang, G.B., Ladow, E.S., Shoenfeld, L.R., Atallah, B.V., Finkbeiner, S., Kreitzer, A.C., 2011. Rapid target-specific remodeling of fast-spiking inhibitory circuits after loss of dopamine. Neuron 71, 858–868.
Goldberg, J.A., Rokni, U., Boraud, T., Vaadia, E., Bergman, H., 2004. Spike synchronization in the cortex/basal-ganglia networks of Parkinsonian primates reflects global dynamics of the local field potentials. J. Neurosci. 24, 6003–6010.
Gruber, A.J., Hussain, R.J., O'Donnell, P., 2009. The nucleus accumbens: a switchboard for goal-directed behaviors. PLoS One 4, e5062.
Guehl, D., Pessiglione, M., François, C., Yelnik, J., Hirsch, E.C., Féger, J., Tremblay, L., 2003. Tremor-related activity of neurons in the 'motor' thalamus: changes in firing rate and pattern in the MPTP vervet model of parkinsonism. Eur. J. Neurosci. 17, 2388–2400.
Halliday, D.M., Rosenberg, J.R., Amjad, A.M., Breeze, P., Conway, B.A., Farmer, S.F., 1995. A framework for the analysis of mixed time series/point process data—theory and application to the study of physiological tremor, single motor unit discharges and electromyograms. Prog. Biophys. Mol. Biol. 64, 237–278.
Hammond, C., Bergman, H., Brown, P., 2007. Pathological synchronization in Parkinson's disease: networks, models and treatments. Trends Neurosci. 30, 357–364.
Higley, M.J., Sabatini, B.L., 2010. Competitive regulation of synaptic Ca2 + influx by D2 dopamine and A2A adenosine receptors. Nat. Neurosci. 13, 958–966.
Hutchison, W.D., Lozano, A.M., Tasker, R.R., Lang, A.E., Dostrovsky, J.O., 1997. Identification and characterization of neurons with tremor-frequency activity in human globus pallidus. Exp. Brain Res. 113, 557–563.
Hutchison, W.D., Allan, R.J., Opitz, H., Levy, R., Dostrovsky, J.O., Lang, A.E., Lozano, A.M., 1998. Neurophysiological identification of the subthalamic nucleus in surgery for Parkinson's disease. Ann. Neurol. 44, 622–628.
Kasanetz, F., Riquelme, L.A., Murer, M.G., 2002. Disruption of the two-state membrane potential of striatal neurones during cortical desynchronisation in anaesthetized rats. J. Physiol. 543, 577–589.
Kravitz, A.V., Freeze, B.S., Parker, P.R., Kay, K., Thwin, M.T., Deisseroth, K., Kreitzer, A.C., 2010. Regulation of parkinsonian motor behaviours by optogenetic control of basal ganglia circuitry. Nature 466, 622–626.
Kreitzer, A.C., Malenka, R.C., 2007. Endocannabinoid-mediated rescue of striatal LTD and motor deficits in Parkinson's disease models. Nature 445, 643–647.
Kühn, A.A., Trottenberg, T., Kivi, A., Kupsch, A., Schneider, G.H., Brown, P., 2005. The relationship between local field potential and neuronal discharge in the subthalamic nucleus of patients with Parkinson's disease. Exp. Neurol. 194, 212–220.
Kumar, A., Cardanobile, S., Rotter, S., Aertsen, A., 2011. The role of inhibition in generating and controlling Parkinson's disease oscillations in the Basal Ganglia. Front. Syst. Neurosci. 5, 86.
Kwak, Y., Peltier, S., Bohnen, N.I., Müller, M.L., Dayalu, P., Seidler, R.D., 2010. Altered resting state cortico-striatal connectivity in mild to moderate stage Parkinson's disease. Front. Syst. Neurosci. 4, 143.
Leblois, A., Boraud, T., Meissner, W., Bergman, H., Hansel, D., 2006. Competition between feedback loops underlies normal and pathological dynamics in the basal ganglia. J. Neurosci. 26, 3567–3583.
Lenz, F.A., Tasker, R.R., Kwan, H.C., Schnider, S., Kwong, R., Murayama, Y., Dostrovsky, J.O., Murphy, J.T., 1988. Single unit analysis of the human ventral thalamic nuclear group: correlation of thalamic "tremor cells" with the 3–6 Hz component of parkinsonian tremor. J. Neurosci. 8, 754–764.
Levy, R., Hutchison, W.D., Lozano, A.M., Dostrovsky, J.O., 2000. High-frequency synchronization of neuronal activity in the subthalamic nucleus of parkinsonian patients with limb tremor. J. Neurosci. 20, 7766–7775.
Levy, R., Hutchison, W.D., Lozano, A.M., Dostrovsky, J.O., 2002. Synchronized neuronal discharge in the basal ganglia of parkinsonian patients is limited to oscillatory activity. J. Neurosci. 22, 2855–2861.
Liu, X.Y., Chu, X.P., Mao, L.M., Wang, M., Lan, H.X., Li, M.H., Zhang, G.C., Parelkar, N.K., Fibuch, E.E., Haines, M., Neve, K.A., Liu, F., Xiong, Z.G., Wang, J.Q., 2006. Modulation of D2R-NR2B interactions in response to cocaine. Neuron 52, 897–909.
Magill, P.J., Bolam, J.P., Bevan, M.D., 2000. Relationship of activity in the subthalamic nucleus-globus pallidus network to cortical electroencephalogram. J. Neurosci. 20, 820–833.
Magill, P.J., Bolam, J.P., Bevan, M.D., 2001. Dopamine regulates the impact of the cerebral cortex on the subthalamic nucleus-globus pallidus network. Neuroscience 106, 313–330.
Mahon, S., Vautrelle, N., Pezard, L., Slaght, S.J., Deniau, J.M., Chouvet, G., Charpier, S., 2006. Distinct patterns of striatal medium spiny neuron activity during the natural sleep–wake cycle. J. Neurosci. 26, 12587–12595.
Mallet, N., Ballion, B., Le Moine, C., Gonon, F., 2006. Cortical inputs and GABA interneurons imbalance projection neurons in the striatum of parkinsonian rats. J. Neurosci. 26, 3875–3884.
Mallet, N., Pogosyan, A., Márton, L.F., Bolam, J.P., Brown, P., Magill, P.J., 2008. Parkinsonian beta oscillations in the external globus pallidus and their relationship with subthalamic nucleus activity. J. Neurosci. 28, 14245–14258.
McCarthy, M.M., Moore-Kochlacs, C., Gu, X., Boyden, E.S., Han, X., Kopell, N., 2011. Striatal origin of the pathologic beta oscillations in Parkinson's disease. Proc. Natl. Acad. Sci. U. S. A. 108, 11620–11625.
Moran, A., Bergman, H., Israel, Z., Bar-Gad, I., 2008. Subthalamic nucleus functional organization revealed by parkinsonian neuronal oscillations and synchrony. Brain 131, 3395–3409.
Moran, R.J., Mallet, N., Litvak, V., Dolan, R.J., Magill, P.J., Friston, K.J., Brown, P., 2011. Alterations in brain connectivity underlying Beta oscillations in parkinsonism. PLoS Comput. Biol. 7, e1002124.
O'Donnell, P., Grace, A.A., 1995. Synaptic interactions among excitatory afferents to nucleus accumbens neurons: hippocampal gating of prefrontal cortical input. J. Neurosci. 15, 3622–3639.
Paxinos, G., Watson, C., 1997. The rat brain in stereotaxic coordinates, 3 rd Edn. Academic Press, London.

Pomata, P.E., Belluscio, M.A., Riquelme, L.A., Murer, M.G., 2008. NMDA receptor gating of information flow through the striatum in vivo. J. Neurosci. 28, 13384–13389.
Quiroga, R.Q., Nadasdy, Z., Ben-Shaul, Y., 2004. Unsupervised spike detection and sorting with wavelets and superparamagnetic clustering. Neural Comput. 16, 1661–1687.
Raz, A., Vaadia, E., Bergman, H., 2000. Firing patterns and correlations of spontaneous discharge of pallidal neurons in the normal and the tremulous 1-methyl-4-phenyl-1,2,3,6-tetrahydropyridine vervet model of parkinsonism. J. Neurosci. 20, 8559–8571.
Rodriguez-Oroz, M.C., Rodriguez, M., Guridi, J., Mewes, K., Chockkman, V., Vitek, J., DeLong, M.R., Obeso, J.A., 2001. The subthalamic nucleus in Parkinson's disease: somatotopic organization and physiological characteristics. Brain 124, 1777–1790.
Rosin, B., Slovik, M., Mitelman, R., Rivlin-Etzion, M., Haber, S.N., Israel, Z., Vaadia, E., Bergman, H., 2011. Closed-loop deep brain stimulation is superior in ameliorating parkinsonism. Neuron 72, 370–384.
Shen, W., Flajolet, M., Greengard, P., Surmeier, D.J., 2008. Dichotomous dopaminergic control of striatal synaptic plasticity. Science 321, 848–851.
Stanford, I.M., 2003. Independent neuronal oscillators of the rat globus pallidus. J. Neurophysiol. 89, 1713–1717.
Steriade, M., McCormick, D.A., Sejnowski, T.J., 1993. Thalamocortical oscillations in the sleeping and aroused brain. Science 262, 679–685.
Steriade, M., Timofeev, I., Grenier, F., 2001. Natural waking and sleep states: a view from inside neocortical neurons. J. Neurophysiol. 85, 1969–1985.
Stern, E.A., Jaeger, D., Wilson, C.J., 1998. Membrane potential synchrony of simultaneously recorded striatal spiny neurons in vivo. Nature 394, 475–478.
Stoffers, D., Bosboom, J.L., Deijen, J.B., Wolters, E.C., Berendse, H.W., Stam, C.J., 2007. Slowing of oscillatory brain activity is a stable characteristic of Parkinson's disease without dementia. Brain 130, 1847–1860.
Terman, D., Rubin, J.E., Yew, A.C., Wilson, C.J., 2002. Activity patterns in a model for the subthalamopallidal network of the basal ganglia. J. Neurosci. 22, 2963–2976.
Tseng, K.Y., Kasanetz, F., Kargieman, L., Riquelme, L.A., Murer, M.G., 2001. Cortical slow oscillatory activity is reflected in the membrane potential and spike trains of striatal neurons in rats with chronic nigrostriatal lesions. J. Neurosci. 21, 6430–6439.
Walters, J.R., Hu, D., Itoga, C.A., Parr-Brownlie, L.C., Bergstrom, D.A., 2007. Phase relationships support a role for coordinated activity in the indirect pathway in organizing slow oscillations in basal ganglia output after loss of dopamine. Neuroscience 144, 762–776.
Zold, C.L., Ballion, B., Riquelme, L.A., Gonon, F., Murer, M.G., 2007a. Nigrostriatal lesion induces D2-modulated phase-locked activity in the basal ganglia of rats. Eur. J. Neurosci. 25, 2131–2144.
Zold, C.L., Larramendy, C., Riquelme, L.A., Murer, M.G., 2007b. Distinct changes in evoked and resting globus pallidus activity in early and late Parkinson's disease experimental models. Eur. J. Neurosci. 26, 1267–1279.